Nuclear Instruments and Methods in Physics Research B

Electron Beam Excitation of Coherent Sub-Terahertz Radiation in Periodic Structures Manufactured by 3D Printing

A.R. Phipps [a], A.J. MacLachlan [a], C.W. Robertson [a], L. Zhang[a], I.V. Konoplev [b], A.W. Cross [a], A.D.R. Phelps [a,*]

[a] *Department of Physics, SUPA, University of Strathclyde, Glasgow, G4 ONG, UK*

[b] *John Adams Institute, Department of Physics, University of Oxford, Oxford, OX1 3RH, UK*

ABSTRACT

For the creation of novel coherent sub-THz sources excited by electron beams there is a requirement to manufacture intricate periodic structures to produce and radiate electromagnetic fields. The specification and the measured performance is reported of a periodic structure constructed by additive manufacturing and used successfully in an electron beam driven sub-THz radiation source. Additive manufacturing, or "3D printing", is promising to be quick and cost-effective for prototyping these periodic structures

Keywords: Periodic structures, electron beam, sub-terahertz radiation, 3D printing

1. Introduction

Additive manufacturing [1], or "3D printing", is a quick and cost-effective method for prototyping periodic structures. In the present work the technical performance of a periodic structure manufactured by 3D printing is reported. The structure reported here has been used in an electron beam driven radiation source that has produced mm-wave output in the 80-90 GHz region. French and Shiffler [2] have reported successfully creating a powerful microwave source in the 4-5 GHz range using 3D printing. Such structures are of great interest because the application of smart electromagnetic designs is having a positive impact on research leading to improved high-power coherent microwave, mm-wave and sub-THz electron-beam-driven sources including both fast wave and slow wave interactions [3-12]. Macor et al. [13] have demonstrated the capability of constructing a variety of passive components for millimetre to terahertz electromagnetic waves, using metal-coated polymers shaped by 3D stereolithography, which uses essentially the same methodology as additive manufacturing, or 3D printing.

One of the motivations for our present research is to explore the range of source frequencies for which 3D printing manufacturing methods for active components can be usefully applied. The dimensional precision that 3D printing can achieve is tending to improve, which should lead to the widening of the frequency range for which this constructional method of producing complex microwave/mm-wave source structures can be applied.

2. Two dimensional (2D) periodic surface lattice (PSL)

The 2D PSLs [14] can be created by manufacturing shallow periodic perturbations on the inner surface of a hollow electrically conducting cylinder. The cylindrical PSL structures need to be compatible with vacuum conditions and the use of energetic electron beams, while also providing the required boundary conditions for the electromagnetic fields. Manufacturing the cylindrical PSLs out of a suitable metal usually provides a good vacuum envelope and the good electrical conductivity allows conduction away of any electrical charges impacting on the surfaces. A good thermal conductivity coefficient is another property that metals tend to possess and is helpful for PSLs intended for use in high power sources.

* Corresponding author.
E-mail address: a.d.r.phelps@strath.ac.uk (A.D.R. Phelps).

The interactions between charged particle beams and periodic structures, that can be one, two, or three dimensional provide a very fruitful research area [15, 16]. Structures used to excite Smith-Purcell radiation share many of the same modeling [16], constructional and measurement challenges as the present work. Periodic structures that produce electromagnetic radiation can be used for several applications that exploit a variety of physical phenomena [17]. A dispersion relation describing the coupling of the volume and surface fields inside a 2D PSL of cylindrical topology was derived by Konoplev et al. [18]. Under certain conditions, when driven by a suitable electron beam this structure can support a Cherenkov instability that provides a coherent source of electromagnetic radiation [19].

The cylindrical 2D periodic structure can be described by equation (1)

$$r = r_0 + \Delta r cos(kz + m\varphi) \qquad (1)$$

where r_0 is the radius of the unperturbed waveguide, Δr is the corrugation depth, $k_z = 2\pi/d_z$, d_z is the period of the corrugation over the z - coordinate and m is the number of variations of the corrugation over the azimuthal coordinate.

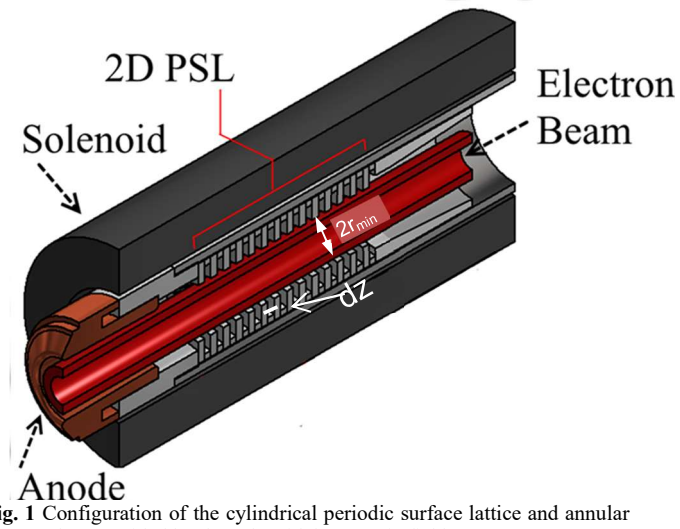

Fig. 1 Configuration of the cylindrical periodic surface lattice and annular electron beam guided by the solenoidal magnetic field.

3. 3D printing of cylindrical 2D PSL

Periodic structures in cylindrical geometry have been successfully prototyped using 3D printing to create a primary mould, which has then been used to cast successfully a metallic cylindrical PSL to form the interaction cavity for a novel sub-THz source.

The 3D printing process is a two stage process. The first stage involves creating a wax former to the 10's of microns scale and then using this former to create a mould for the component where the silver – chromium molten alloy is deposited, with the resulting part having a resolution of ± 125 microns. The PSL to be used in the 'hot' experiment was constructed using a high resolution 3D printing process that included the injection moulding of a silver chromium alloy. 3D printing, originally developed in the mid 1980's , offers the possibility of producing objects that have resolutions on the 10's of microns scale. 3D printing is an additive process by which consecutive layers in the x-z plane are deposited sequentially in the positive y direction (upwards), resulting in a high resolution (approximately ± 15 microns) wax model that is then used in a casting process that ultimately results in the silver alloy (80 to 90) GHz 2D PSL, seen in the image below. The printing process follows the pattern in a given CAD input file, usually in the STL (Stereolithograph) file format where every face is built from a series of interconnected triangles represented by 3 separate 32-bit floating-point Cartesian coordinates. More often now the new X3D file format is implemented which incorporates the XML programming interface and further enhancements over its predecessors. The design is sliced into digital layers so that a curve is 'approximated' by many square sided slices, with the thickness of each layer representing the resolution of that particular 3D printing process.

Although this resolution is not at present as high as can be achieved with a precision milling process, it does have the advantage of taking a lot less time to achieve the finished structure and in conjunction with the lower cost, the 3D printing process is more efficient overall.

A 2D PSL structure with parameters as shown in Table 1 was manufactured for electromagnetic measurements using a VNA and for subsequent use in electron beam experiments. Images of the cylindrical 2D PSL made using 3D printing are shown in Fig. 2.

Fig. 2. Cylindrical PSL manufactured using 3D printing.

Parameter	Symbol	Value
Longitudinal Period	dz	1.6 mm
Azimuthal Variations	m	7
Number of Longitudinal Periods	n	16
Amplitude	dr	0.8 mm
Amplitude (Peak-to-Peak)	dr (pk-pk)	1.6mm
Inner Radius of input and output waveguide	r	4 mm
Minimum radius of perturbation (ID)	r_{min}	3.6 mm
Mean radius	r_0	4.4 mm
Maximum radius of perturbation (OD)	r_{max}	5.2 mm

Table 1. The physical parameters of the 2D PSL structure

The 2D cylindrical PSL shown in Fig. 2 is made from a silver alloy of 92.5% silver and 7.5% chromium.

4. Electromagnetic measurement of the cylindrical 2D PSL

Measurements, made using a vector network analyser, of the electromagnetic properties of the cylindrical PSL manufactured by these methods, are compared with simulations made using the software CST Microwave Studio.

Using a serpentine co-axial mode converter operating in G-band (140GHz to 220GHz) a $TM_{0,n}$ wave was launched into the high contrast (1.6 mm deep corrugation) 2D PSL with the transmission measured over the 140GHz to 220GHz frequency range using an Anritsu ME7808B Broadband Lightening Vector Network Analyzer VNA with two transmit and receive SM5952 140-220 GHz OML extender heads. The $TM_{0,1}$ mode from the circular serpentine mode converter becomes a TEM mode in the co-axial conical horn which then launches a $TM_{0,n}$ mode in the cylindrical 3D printed 2D PSL.

When testing the structure using the VNA the interaction produces an electromagnetic wave that interacts with the 1.6mm longitudinal period giving a response in G-band resulting in a resonance at 187.7GHz, as shown in figure 3 showing the millimetre wave transmission as a function of frequency. The electromagnetic wave when interacting with the 3.5 mm azimuthal period will give a fundamental resonance at ~85 GHz and a resonance at the 1st harmonic in G-band. The latter is considered to give rise to the 171.1GHz resonance in G-band shown in the VNA measurement.

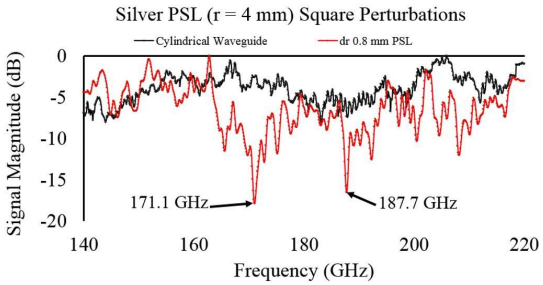

Fig. 3. The measured transmission as a function of frequency of the 2D PSL over the 140 GHz to 220 GHz frequency range.

5. Electron beam interaction with the cylindrical 2D PSL

Parameter	Symbol	Value
Accelerating potential	V	80 kV
Axial velocity	v_z	0.46c
Perpendicular velocity	v_{perp}	0.19c
Lorentz factor	γ	1.156
Maximum current	I_{max}	100A
Applied axial magnetic field	B	1.8T
Electron beam radius	R_{beam}	2.0 mm

Table 2. The parameters of the electron beam

For an electron beam with the parameters as shown in Table 2, having an accelerating potential of 80 kV, and $v_z = 0.46c$, interacting with the cylindrical 2D PSL structure for which dz= 1.6 mm, equation (2) indicates the electrons will interact with a localized surface field at a frequency of ~ 85 GHz

$$\omega = k_z v_z \pm \frac{2\pi}{d_z} v_z \sim 85\ \text{GHz} \qquad (2)$$

This matches with the electromagnetic wave fundamental resonance in the azimuthal direction of ~85 GHz

6. Electron beam experiments and mm-wave output measurements

The cylindrical 2D PSL was assembled with the electron gun and output waveguide and window. The cylindrical 2D PSL was located inside a water-cooled solenoidal electromagnet that was capable of providing a uniform axial magnetic field of up to 2T over the axial extent of the 2D PSL, as shown in Fig. 1. An axial magnetic field of 1.8T was used in the experiments reported here. A two stage vacuum pumping system was used to evacuate the integrated system to a pressure of ~ 1 x 10^{-6} mbar which was sufficient for short pulse (~100ns) cold cathode electron beam production. The complete experimental assembly is shown in Fig. 4.

Measurements of the magnetic field profile, electron beam accelerating

potential, beam current, electron beam profile and output millimetre wave radiation have been carried out. A pulsed power supply capable of providing up to 100kV peak voltage pulses was applied to a vacuum diode and an electron beam was extracted from a cold cathode. A measurement of the accelerating potential and the electron beam current is shown in Fig. 5. A witness plate diagnostic was used to record the cross-sectional profile of the electron beam. The measured cross-sectional beam profile appears to be annular [20], which is ideal, although the optimum configuration would be for the beam to pass even closer to the surface of the 2D PSL The 80 kV, 100 A electron beam was measured to have a beam radius of 2.0 mm which was approximately 1.6 mm away from the inner surface of the 2D PSL corrugation. The pulse repetition frequency is very low and the experiment is effectively 'single shot'. No changes in the radiated sub-THz radiation and no changes in the properties of the PSL were observed during these experiments, indicating no significant damage of the PSL. It is planned to reduce the distance between the electron beam and the inner surface of the 2D PSL in a future series of experiments to further strengthen the electron beam 2D PSL interaction.

At the relatively low electron beam energies (< 100 keV) used in these experiments the applied axial magnetic field of up to 2T is able to guide the electron trajectories. The alignment of the electron beam with the axis of the PSL depends both on good mechanical alignment and on alignment of the axis of the magnetic field. The radiation produced by the interaction of the electron beam with the PSL propagates within a conducting waveguide towards the output window. Radiation directivity effects produced by any misalignment of the electron beam and the PSL tend to be masked by the sub-THz radiation propagation through the conducting waveguide.

The millimetre wave radiation was measured using a rectifying crystal detector with the output mode pattern recorded by scanning the crystal detector across the output window and plotting the magnitude of the millimetre wave pulse as a function of angle. Initial measurements of the radiation pattern have been made. It is expected that the PSL should produce a coupling of a $TM_{0,2}$ field and a $TE_{5,1}$ field. The radiation pattern measurements are not inconsistent with this expectation but further measurements are needed before a firm identification is established."

The frequency of the millimetre wave radiation was measured using a series of high pass cut-off filters in combination with the millimetre wave crystal detector with the mode pattern measured in the far field. The use of the series of cut-off filters shows that millimetre wave output is being successfully generated as show in Fig. 6 and that this millimetre wave output lies between 80 GHz and 85 GHz. A more accurate frequency measurement in the form of a heterodyne frequency diagnostic will be used as part of our future work.

The measured peak power was estimated to be approximately 30kW. The relatively low efficiency, of less than 1%, is considered to be a result of the electron beam not passing close enough to the PSL structure.

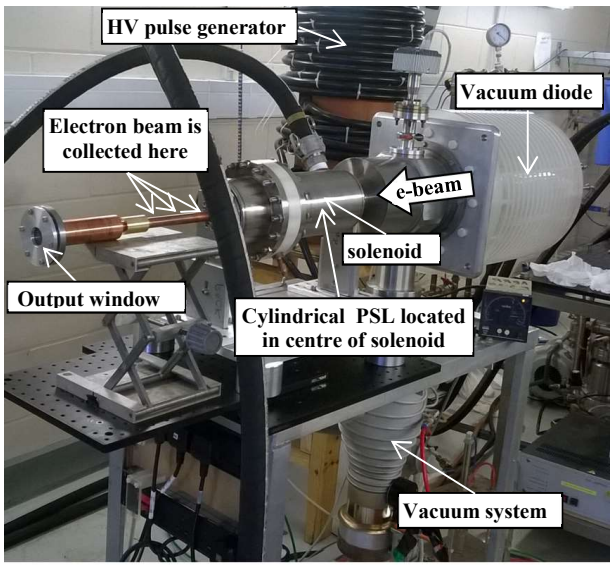

Fig. 4 Complete experimental assembly showing the vacuum diode source of the electron beam, the magnetic field solenoid surrounding the cylindrical 2D PSL and the output window.

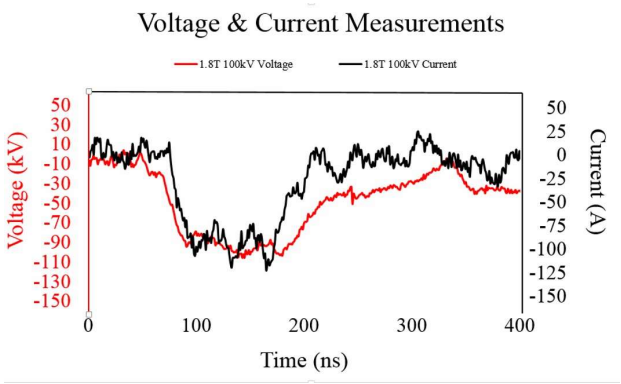

Fig. 5. The beam current and accelerating voltage seen at the cathode. A value of 80 kV produced a current of approximately 100 A

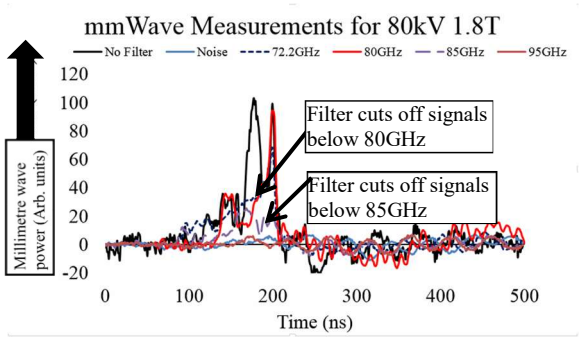

Fig. 6. Millimetre wave output and frequency diagnostic.

7. Conclusions

The magnetic field solenoid creates an applied, guiding axial magnetic field in these experiments, in the region where the electron beam is interacting with the electromagnetic fields of the PSL. This applied magnetic field then decreases by several orders of magnitude in the region just downstream of the PSL. The result of this is that the electrons follow the magnetic field lines and move out radially and are collected on the conducting wall of the vacuum vessel downstream of the PSL. The electron trajectories have also been numerically modelled and a negligible number of electrons are predicted to impact on the output window. The experimental observations are consistent with this. In practical applications to produce radiation using PSLs, bremsstrahlung production in the output window should not pose a significant risk.

The construction and operation of an electron beam driven millimetre wave source based on a cylindrical 2D PSL has been achieved and the millimetre wave output has been measured. A novel feature of this result is that the 2D PSL has been constructed using 3D printing. Sources in the microwave frequency range have only relatively rarely been constructed previously using 3D printing. As the wavelength decreases the need for higher precision increases and the results reported here have extended the applicability of 3D printing as a construction method into the millimetre wave range.

Acknowledgements

This project has received funding from the Leverhulme Trust through an International Network Grant IN-2015-012. The research effort has been supported by AFOSR through award number FA8655-13-1-2132. Alan Phipps and Amy MacLachlan thank the EPSRC UK for funding their PhD studentships.

References

[1] I. Gibson, D. Rosen, B. Stucker, Additive manufacturing technologies : 3D printing, rapid prototyping, and direct digital manufacturing, 2nd ed., Springer, New York, NY, USA, 2015.
[2] D.M. French, D. Shiffler, High power microwave source with a three dimensional printed metamaterial slow-wave structure, Rev. Sci. Instrum., 87 (2016) 053308.

[3] N.S. Ginzburg, N.Y. Peskov, A.S. Sergeev, et al., Theory of free-electron maser with two-dimensional distributed feedback driven by an annular electron beam, J. Appl. Phys., 92 (2002) 1619-1629.
[4] N.S. Ginzburg, N.Y. Peskov, A.S. Sergeev, et al., The use of a hybrid resonator consisting of one-dimensional and two-dimensional Bragg reflectors for generation of spatially coherent radiation in a coaxial free-electron laser, Phys. Plasmas, 9 (2002) 2798-2802.
[5] I.V. Konoplev, P. McGrane, A.W. Cross, et al., Wave interference and band gap control in multiconductor one-dimensional Bragg structures, J. Appl. Phys., 97 (2005) 073101.
[6] I.V. Konoplev, A.W. Cross, A.D.R. Phelps, et al., Experimental and theoretical studies of a coaxial free-electron maser based on two-dimensional distributed feedback, Phys. Rev. E, 76 (2007) 056406.
[7] I.V. Konoplev, L. Fisher, A.W. Cross, et al., Excitation of surface field cavity and coherence of electromagnetic field scattering on two-dimensional cylindrical lattice, Appl. Phys. Lett., 97 (2010) 261102.
[8] I.V. Konoplev, L. Fisher, K. Ronald, et al., Surface-field cavity based on a two-dimensional cylindrical lattice, Appl. Phys. Lett., 96 (2010) 231111.
[9] I.V. Konoplev, A.R. Phipps, A.D.R. Phelps, et al., Surface field excitation by an obliquely incident wave, Appl. Phys. Lett., 102 (2013) 141106.
[10] N.S. Ginzburg, A.S. Sergeev, N.Y. Peskov, et al., Mode competition and control in free electron lasers with one- and two-dimensional Bragg resonators, IEEE Trans. Plasma Sci., 24 (1996) 770-780.
[11] A.W. Cross, W. He, I.V. Konoplev, et al., Experimental and theoretical study of 2D Bragg structures for a coaxial free electron maser, Nucl. Instrum. Methods Phys. Res. Sect. A-Accel. Spectrom. Dect. Assoc. Equip., 475 (2001) 164-172.
[12] A.W. Cross, I.V. Konoplev, K. Ronald, et al., Experimental studies of two-dimensional coaxial Bragg structures for a high-power free-electron maser, Appl. Phys. Lett., 80 (2002) 1517-1519.
[13] A. Macor, E. de Rijk, S. Alberti, et al., Note: Three-dimensional stereolithography for millimeter wave and terahertz applications, Rev. Sci. Instrum., 83 (2012) 046103.
[14] I.V. Konoplev, L. Fisher, A.W. Cross, et al., Surface wave Cherenkov maser based on a periodic lattice, Appl. Phys. Lett., 96 (2010) 261101.
[15] M. Shevelev, A. Konkov, A. Aryshev, Soft-x-ray Cherenkov radiation generated by a charged particle moving near a finite-size screen, Phys. Rev. A, 92 (2015) 14.
[16] K. Lekomtsev, P. Karataev, A.A. Tishchenko, et al., CST simulations of THz Smith-Purcell radiation from a lamellar grating with vacuum gaps, Nucl. Instrum. Methods Phys. Res. Sect. B-Beam Interact. Mater. Atoms, 355 (2015) 164-169.
[17] A.W. Cross, I.V. Konoplev, A.D.R. Phelps, et al., Studies of surface two-dimensional photonic band-gap structures, J. Appl. Phys., 93 (2003) 2208-2218.
[18] I.V. Konoplev, A.J. MacLachlan, C.W. Robertson, et al., Cylindrical, periodic surface lattice-Theory, dispersion analysis, and experiment, Appl. Phys. Lett., 101 (2012) 121111.
[19] I.V. Konoplev, A.J. MacLachlan, C.W. Robertson, et al., Cylindrical periodic surface lattice as a metadielectric: Concept of a surface-field Cherenkov source of coherent radiation, Phys. Rev. A, 84 (2011) 013826.
[20] I.V. Konoplev, A.W. Cross, P. MacInnes, et al., High-current oversized annular electron beam formation for high-power microwave research, Appl. Phys. Lett., 89 (2006) 171503.